



HAL
open science

Genomes and integrative genomic insights into the genetic architecture of main agronomic traits in the edible cherries

Zhenshan Liu, Anthony Bernard, Yan Wang, Elisabeth Dirlewanger, Xiaorong Wang

► **To cite this version:**

Zhenshan Liu, Anthony Bernard, Yan Wang, Elisabeth Dirlewanger, Xiaorong Wang. Genomes and integrative genomic insights into the genetic architecture of main agronomic traits in the edible cherries. *Horticulture research*, 2024, 12, <10.1093/hr/uhae269>. <hal-04881952>

HAL Id: hal-04881952

<https://hal.inrae.fr/hal-04881952v1>

Submitted on 13 Jan 2025

HAL is a multi-disciplinary open access archive for the deposit and dissemination of scientific research documents, whether they are published or not. The documents may come from teaching and research institutions in France or abroad, or from public or private research centers.


L'archive ouverte pluridisciplinaire **HAL**, est destinée au dépôt et à la diffusion de documents scientifiques de niveau recherche, publiés ou non, émanant des établissements d'enseignement et de recherche français ou étrangers, des laboratoires publics ou privés.



Distributed under a Creative Commons CC BY 4.0 - Attribution - International License

Review Article

Genomes and integrative genomic insights into the genetic architecture of main agronomic traits in the edible cherries

Zhenshan Liu¹, Anthony Bernard ², Yan Wang^{1,3}, Elisabeth Dirlwanger^{2,*} and Xiaorong Wang^{1,3,*}

¹College of Horticulture, Sichuan Agricultural University, Chengdu 611130, China

²INRAE, Univ. Bordeaux, UMR BFP, Villenave d'Ornon 33882, France

³Key Laboratory of Agricultural Bioinformatics, Ministry of Education, Chengdu 611130, China

*Corresponding authors. E-mails: elisabeth.dirlwanger@inrae.fr; wangxr@sicau.edu.cn

Abstract

Cherries are one of the economically important fruit crops in the Rosaceae family, *Prunus* genus. As the first fruits of the spring season in the northern hemisphere, their attractive appearance, intensely desirable tastes, high nutrients content, and consumer-friendly size captivate consumers worldwide. In the past 30 years, although cherry geneticists and breeders have greatly progressed in understanding the genetic and molecular basis underlying fruit quality, adaptation to climate change, and biotic and abiotic stress resistance, the utilization of cherry genomic data in genetics and molecular breeding has remained limited to date. Here, we thoroughly investigated recent discoveries in constructing genetic linkage maps, identifying quantitative trait loci (QTLs), genome-wide association studies (GWAS), and validating functional genes of edible cherries based on available *de novo* genomes and genome resequencing data of edible cherries. We further comprehensively demonstrated the genetic architecture of the main agronomic traits of edible cherries by methodically integrating QTLs, GWAS loci, and functional genes into the identical reference genome with improved annotations. These collective endeavors will offer new perspectives on the availability of sequence data and the construction of an interspecific pangenome of edible cherries, ultimately guiding cherry breeding strategies and genetic improvement programs, and facilitating the exploration of similar traits and breeding innovations across *Prunus* species.

Introduction

Cherry trees are one of the most representative economically important members of the family Rosaceae genus *Prunus*, which contains many famous stone fruits like almonds, apricots, peaches, plums, etc. [1]. Cherry trees include various species valued for three major purposes: as edible fruits for fresh eating or processing like sweet cherry (*Prunus avium* L., syn. *Cerasus avium* (L.) Moench, $2n=2x=16$), Chinese cherry (*Prunus pseudocerasus* Lindl., syn. *Cerasus pseudocerasus* (Lindl.) G.Don, $2n=4x=32$), sour/tart cherry (*Prunus cerasus* L., syn. *Chlorella vulgaris* Mill., $2n=4x=32$), and Nanking cherry (*Prunus tomentosa* Thunb., syn. *Cerasus tomentosa* (Thunb.) Wall., $2n=2x=16$), as rootstocks like *Prunus mahaleb* L. (syn. *Cerasus mahaleb* (L.) Mill.), and as blooming ornamentals like *Prunus serrulata* Lindl. (syn. *Cerasus serrulata* (Lindl.) G.Don ex London) [2–4]. In 2022, cherries were grown on 454 664 hectares with a total production of 2 765 827 tons worldwide, with Turkey and China being the largest producer and importer, respectively (www.fao.org/faostat/en/).

There is a large phenotypic variability and genetic diversity among these edible cherries. Sweet cherry is characterized by high fruit weight, large edible proportion, high sugar content, and low acidity, making it suitable for fresh eating [5]. Sour cherry is rich in acids and is valued for superior characteristics in pro-

cessed products, such as juice, compote, jam, and pie filling [6]. Both sweet and sour cherries are believed to have originated in Europe around the Caspian and Black Seas, with the Caucasus area considered a major center of genetic diversity [7, 8]. Chinese cherry, native to China with wide natural distributions in South China, is characterized by full-flavored but small fruits [9, 10], and contains a diverse range of flavonols, especially kaempferol glycosides and quercetin glycosides [2, 11]. Nanking cherry, native to China, exhibits great adaptability to various environments, with fruits characterized by high total phenolic content (especially flavonols and tannins) and high antioxidant activity [2, 12].

In the last 30 years, breeders worldwide have been working on edible cherries improvement, focusing on fruit quality determining marketability, phenological phases better adapted to climate change, and other high-impact stakeholder-driven production traits such as disease resistance [3, 13–15]. For sweet cherry, hundreds of cultivars are available for growers, with the number of commercial cultivars increasing notably in recent decades [3]. Moreover, a large diversity of cherry landraces are conserved in Genetic Resources Centers (GRCs), such as Cherry Germplasm Repository (Chengdu, China), which mainly conserves Chinese cherry resources, and *Prunus* GRC of INRAE at Bourran (Lot and Garonne, France), which mainly conserves sweet cherry resources,

Received: 25 July 2024; Accepted: 17 September 2024; Published: 24 September 2024; Corrected and Typeset: 1 January 2025

© The Author(s) 2024. Published by Oxford University Press on behalf of Nanjing Agricultural University. This is an Open Access article distributed under the terms of the Creative Commons Attribution License (<https://creativecommons.org/licenses/by/4.0/>), which permits unrestricted reuse, distribution, and reproduction in any medium, provided the original work is properly cited.

and many have been used for production at a local level, or more recently in modern breeding programs [16].

Breeding has been widely leveraged in many crops for yielding hybrid heterosis [17, 18]. However, high heterozygosity and polygenic control of economically important traits make the dissection of genetic architecture difficult [19], posing a bigger challenge, exacerbated in perennial woody plants and polyploids such as Chinese cherry and sour cherry. Over the past half-century, the release of high-quality genomes and basic molecular technology has advanced our understanding of important aspects of cherry genetics. This includes the consolidation of the phylogenetic relationships, the analysis of the genetic variability, the development of high-throughput genotyping methods, the construction of genetic linkage maps, and the discovery of major genes and quantitative trait loci (QTLs). The Genome Database for Rosaceae (GDR, <https://www.rosaceae.org>) [20] made all these data publicly available.

Nevertheless, the use of cherry genomic data is still limited to date, although it could help in understanding the genetic and molecular basis underlying fruit quality, adaptation to climate change, and disease/pest resistance. In this review, we [21] track recent cherry genome achievements and single-nucleotide polymorphism (SNP) arrays, and [19] investigate the trait heredity in genome-wide association studies (GWAS), construction of genetic linkage maps, the discovery of QTLs, and validation of functional genes, and then systematically integrate QTLs, GWAS loci, and functional genes into an identical reference genome to comprehensively demonstrate the genetic architecture of the main agronomic traits. These collective endeavors offer new perspectives on the biology and trait inheritance of edible cherries, aiding in the discovery of genomic loci that control crucial agronomic traits and the construction of an interspecific pangenome of edible cherries, also facilitating the exploration of similar traits and breeding innovations across *Prunus* species.

Genomic data with SNP arrays of edible cherries

The *de novo* genomes

The basic chromosome (Chr) number for edible cherries is consistent with that of other *Prunus* species, standing at 8. To date, *P. avium*, *P. cerasus*, and *P. pseudocerasus* have been sequenced (Table 1). The first draft genome sequence of the sweet cherry cv. 'Satonishiki' was released in 2017 [22]. It was assembled based on the Illumina platform and showed low heterogeneity. A total of 272.36 Mb in scaffolds were assembled, with an N50 of 0.22 Mb and the longest scaffold of 1.46 Mb, representing 77.8% of the estimated genome size (352.8 Mb). In 2020, three sweet cherry cultivars were sequenced and assembled: cv. 'Tieton' (with two versions of the genome [23, 24], cv. 'Regina' [25] and cv. 'Big Star' [26]. The second version of the sweet cherry cv. 'Tieton' greatly improved quality and completeness by integrating multiple technologies: Oxford Nanopore technology (ONT), short Illumina sequencing, and Hi-C scaffolding. The final *de novo* assembly resulted in a phased haplotype assembly of 344.29 Mb with a contig N50 of 3247.2 kb [23]. Recently, an updated complete genome of chromosome-doubled sweet cherry cv. 'Tieton' was released [27]. Advanced sequencing technology third-generation circular consensus sequencing (CCS) and Hi-C were applied to assemble a high-quality genome with a total size of 341.62 Mb and an N50 length of 39.81 Mb.

Several studies have demonstrated that sour cherry is a natural hybrid derived from a tetraploid resembling *Prunus fruticosa*

(ground cherry) and a diploid resembling *P. avium* [28, 29]. The allotetraploid origin of sour cherry is well established and further supported by the recently published genome: Sour cherry cv. 'Montmorency' is trigonomic, containing two distinct subgenomes inherited from ground cherry (A and A') and two copies of the same subgenome from sweet cherry (BB) [30]. The genome composition of 'Montmorency' is AA'BB and little-to-no recombination has occurred between the progenitor subgenomes (A/A' and B). A total of 92 783 protein-coding genes were predicted in the full assembly of 'Montmorency' (1066 Mb) with a high Benchmarking Universal Single-Copy Orthologs (BUSCO) completion score of 98.6% [30].

A chromosome-level, haplotype-resolved genome of Chinese cherry cv. 'Zhuji Duanbing' was assembled into 32 pseudochromosomes, 4 haplotypes, comprising 993.69 Mb [31]. Intra-haplotype comparative analyses revealed extensive intra-genomic sequence and expression consistency, confirming that *P. pseudocerasus* was a stable autotetraploid species [4, 32].

Resequencing efforts and SNP arrays

With the advancement of Next-Generation Sequencing, there has been a thriving progression in the development of SNP arrays [33, 34] and ongoing resequencing studies [35–38]. The first 6 K array, led by RosBREED, consisted of 4214 sweet cherry SNPs and 1482 sour cherry SNPs. However, only a third of them were polymorphic in the sweet and sour cherry evaluation panels, with low coverage in many genomic regions. Subsequently, an additional 9 K SNPs were added onto the 6 K array following a focal point strategy, including SNPs from *fruticosa* subgenomes of sour cherry, respectively [34]. The final 15 K SNPs increased genetic resolution and genome coverage, contributing to a better understanding of the genetic control of key traits. The use of RosBREED Cherry 6 + 9 K SNP array allowed the saturation of previously generated SNP maps in the species, revealing a powerful tool for QTL and genetic analysis [40, 39]. As expected, the number of heterozygous SNPs detected by the 15 K array [40] was larger (1.5–1.9 times) than previously observed for the same cultivars ('Vic' and 'Cristobalina') with the 6 K array [41]. In essence, these two arrays lie in a foundational work that has significantly advanced modern molecular breeding research of cherries [43, 42–45]. The first whole-genome resequencing was conducted to characterize genetic variation, population structure, and allelic variants in a panel of 21 sweet cherries, which encompassed the majority of cultivated Greek germplasm and a representative of a local wild cherry elite phenotype [38]. These expanded sequencing datasets, combined with those genomes, greatly increase the value of cherry breeding and advance our understanding of their evolution, diversity, and the genetic control of valuable traits.

Genetics and functional genomics of edible cherries

Development of genetic linkage maps

Genetic linkage maps are composed of molecular markers, the order of which is arranged based on genetic distance estimated from recombination events between individuals. They serve as a powerful tool for exploring and understanding the inheritance of agronomic traits from parents. The history and development of genetic maps for edible cherries are summarized in Table 2, representing the concerted efforts of geneticists and breeders worldwide. Most of the genetic maps are based on the analysis of F₁ populations derived primarily from crosses between sweet

Table 1. Summary of edible cherries genomes assembly.

Species/cultivar: genome version	Estimated genome size (Mb)	Assembled genome size (Mb)	Contig N50 (Mb)	Scaffold N50 (Mb)	Longest scaffold (Mb)	BUSCO (%)	# of genes	Sequencing platform	Reference
<i>P. avium</i> (2n = 2x = 16)									
'Satonishiki'	352.9	272.36	28.779	0.22	1.46	96	43673	Illumina (HiSeq2000)	[22]
'Tieton' V1.0	341.38	280.33	0.064	2.48	17.96	95.9	30975	Illumina (HiSeq X Ten)	[24]
'Tieton' V2.0	340.05	344.29	3.247		/(LG1: 62.32)	97.4	40338	Illumina (HiSeq X Ten) + Nanopore + Hi-C	[23]
'Tieton' T2T		341.62	39.81		/(LG1: 62.94)	98.4	58204	CCS + HiC	[27]
'Regina'	338	279	1.230	~6.00	16.3	95.9	39180	PacBio	[25]
'Big Star'	322	272.05	0.215	0.19	1.38	95.6	29487	Illumina (HiSeq2000)	[26]
<i>P. cerasus</i> (2n = 4x = 32, AA'BB)									
'Montmorency'	621 (haploid)	1066 (subgenomes A, A', B)	11.560		/(LG1A: 52.66)	98.6	92783	Illumina (HiSeq4000) + Pacbio + Nanopore + Hi-C	[30]
<i>P. pseudocerasus</i> (2n = 4x = 32)									
'Zhuji Duanbing' V1.0	1090	359.26	1.11	33.00		97.6	41811	Illumina (HiSeq X Ten) +	[31]
'Zhuji Duanbing' V2.0	1090	994.21 (Hap1: 246.30; Hap2: 237.02; Hap3: 225.52; Hap4: 192.91)	7.05 (Hap1: 7.84, Hap2: 6.85; Hap3: 6.00; Hap4: 5.43)	27.26		98.6 (Hap1: 96.00, Hap2: 93.70; Hap3: 88.60; Hap4: 74.30)	Hap1: 26326, Hap2: 25289; Hap3: 24213; Hap4: 20256	Pacbio + Nanopore + Hi-C	

Note: BUSCO: Benchmarking Universal Single-Copy Orthologs were used to assess the completeness of the assembly.

Table 2. Genetic linkage maps of edible cherries.

Origin/mapping parents	Pop size	Pop type	Number of markers	Marker type	Map size (cM)	Linkage groups	Mean marker interval (cM)	References
<i>P. avium</i>								
'EF'	56	Microspore-derived callus	89	RAPD	503.3	10	5.6	[46]
'Regina' × 'Lapins'	122	F ₁	144	SSR	711.1	8	4.9	[94]
'NY' × 'EF'	86;	F ₁	91	SSR; CAPS; AFLP; SRAP; gene-derived marker	565.8	8	6.2	[95]
'EF' × 'NY'	103	F ₁	50	RAPD; ISSR; SSR	634.67	8	12.7	[96]
'Rainier' × '8-100'	90	F ₁	149	SNP; SSR, Indel, S-Rnase	779.4	8	5.4	[97]
'NY54' × 'EF'; 'Regina' × 'Lapins'; 'Namati' × 'Summit'; 'Namati' × 'Krupnoplodnaya'	424	F ₁	723	SNP	752.9	8	1.1	[47]
'Black Tartarian' × 'Kordia'	89	F ₁	335 (R); 247 (L); 687 (RXL)	SNP	619.4 (R), 610.1 (L), 639.9 (RXL)	8	1.85 (R); 2.47 (L) 0.93 (RXL)	[43]
'Regina' × 'Lapins'	121	F ₁	136 (R); 127 (L)	SNP	712.4 (R); 710.4 (L)	8	5.2 (R); 5.6 (L)	[43]
'Regina' × 'Lapins'	121	F ₁	142 (R); 137 (G)	SNP	657.6 (R); 823.6 (G)	8	4.6 (R); 6.0 (G)	[43]
'Rainier' × 'Rivedel'	117	F ₁	985	SNP; SSR	731.3	8	0.7	[98]
'Wanhongzhu' × 'Lapins'	675	F ₁	718	SNP; SSR; S gene	849	8	1.18	[90]
'Beniyutaka' × 'Benikirari'; 'C-195-50' × 'Benikirari'; 'Nanyo' × 'Benisayaka'	100; 562	F ₁	2382	SNP; SSR	1165	8	0.49	[22]
'Beniyutaka' × 'Benikirari'	94	F ₁	782 (BY); 742 (BK)	SNP; SSR	600.7 (BY); 825.8 (BK)	8	0.77 (BY); 1.11 (BK)	[98]
'C-195-50' × 'Benikirari'	84	F ₁	419 (C-195-50); 625 (BK)	SNP; SSR	745.2 (C-); 926.6 (BK)	8	1.78 (C-); 1.48 (BK)	[98]
'Nanyo' × 'Benisayaka'	304	F ₁	607 (N); 657 (BY)	SNP; SSR	969.3 (N); 1223.5 (BY)	8	1.60 (N); 1.86 (BY)	[41]
'Vic' × 'C'	161	F ₁	816	SNP	726	8	0.9	[41]
'C' × 'C'	97	F ₂	511	SNP	634.1	8	1.7	[41]
'Brooks' × 'C'	67	F ₂	552	SNP	622.4	8	1.2	[41]
'Ferce' × 'X'	67	F ₁	110 (F); 87 (X)	SNP	715 (F); 652.5 (X)	8	6.5 (F); 7.5 (X)	[73]
'Ambrunés' × 'Sweetheart'	140	F ₁	463 (A); 254 (S); 820 (AxS)	SNP	867.8 (A); 529.1 (S); 827.6 (AxS)	8	2.1 (A); 2.4 (S); 1.0 (AxS)	[60]
'Vic' × 'C'; 'Ambrunés' × 'C'; 'Brooks' ('B') × 'C'; 'Lambert' × 'C'; 'C' × 'C'; 'B' × 'C'-F ₂	406;	F ₁ ; F ₂ ('C' × 'C'; 'B' × 'C')	1269	SNP	721.98	8	0.57	[77]
'Vic' × 'C'	161	F ₁	910 (Vic); 789 (C); 2000 (VicxC)	SNP	636.7 (Vic); 666.0 (C); 794.3 (VicxC)	8	0.70 (Vic); 0.84(C); 0.37 (VicxC)	[40]
'Regina' × 'Garnet'	454	F ₁	598 (R); 446 (G)	SNP	614.5 (R); 619 (G)	8	1.1 (R); 1.7 (G)	[39]
	1.386 (fine mapping)	F ₁	17	KASP	0.887 kb (9.269–10.156 kb)*	1 (LCA)	0.052 kb*	[39]

(Continued)

Table 2. Continued

Origin/mapping parents	Pop size	Pop type	Number of markers	Marker type	Map size (cM)	Linkage groups	Mean marker interval (cM)	References
<i>P. cerasus</i>								
'RS' × 'EB'	86	F ₁	126 (RS); 95 (EB)	SDRF	461.6 (RS); 279.2 (EB)	19 (RS); 16 (EB)	3.66 (RS); 2.94 (EB)	[99]
'RS' × 'EB'	86	F ₁	67 (RS); 43 (EB); 80 (RS×EB)	RFLP	398.2 (RS); 222.2 (EB); 272.9 (RS×EB)	15 (RS); 8 (EB); 17 (RS×EB)	9.8 (RS&EB); 4.8 (RS/EB)	[100]
'M172' × '25-02-29'; 'Montmorency' × '25-02-29'; '25-14-20' × '25-02-29'; 'ÚjfehértóFürtös' × 'Surefire'; 'Rheinische Schattenmorelle' × 'Englaise Timpurii'	330	F ₁	2058	SNP	659.5	8	0.3	[48]
<i>P. avium</i> × <i>Prunus incisa</i>								
'Napoleon' × 'E621'	63	F ₁	14	Isoenzyme		4		[101]
<i>P. avium</i> × <i>Psychomyia nipponica</i>								
'Napoleon' × 'F1292'	47	F ₁	14	Isoenzyme		4		[101]
'Napoleon' × 'F1292'	94	F ₁	166	SSR; gene-specific marker	680	8	3.9	[102]

Note: Pop: population; 'EF': Emperor Francis; 'RS': Rheinische Schattenmorelle; EB: Erdi Botermo; NY: New York; 'C': Cristobalina; RAPD: random amplified polymorphic DNA; SDRF: single-dose restriction fragment; RFLP: restriction fragment length polymorphism; SSR: simple sequence repeat; CAPS: cleaved amplified polymorphism sequence; AFLP: amplified fragment length polymorphism; SRAP: sequence-related amplified polymorphism; SNP: single-nucleotide polymorphism; S-gene: self-incompatibility gene. * The 'Map size (cM)' and 'Mean marker interval (cM)' of the 17 KASP markers are given in kilobase pairs (kb) of the physical position on the 'Regina' genome.

cherry accessions. The first genetic map was constructed on sweet cherry using random amplified polymorphic DNA (RAPD) and isoenzyme marker analysis of 56 microspore-derived callus individuals of the cv. 'Emperor Francis' [46]. Prior to the development of the first 6 K SNP array, studies focused on developing and densifying frameworks using long-fragment markers such as simple sequence repeat (SSR), cleaved amplified polymorphism sequence (CAPS), amplified fragment length polymorphism (AFLP), sequence-related amplified polymorphism (SRAP), RAPD, restriction fragment length polymorphism (RFLP), etc. It was not until Klagges *et al.* [47] used two F_1 intra-specific populations of sweet cherry, 'Black Tartarian' \times 'Kordia' (BT \times K) and 'Regina' \times 'Lapins' (R \times L), that two SNP-based highly dense maps consisting of 723 and 687 markers were constructed, containing eight linkage groups spanning 752.9 and 639.9 cM with an average distance of 1.1 and 0.9 cM of BT \times K and R \times L, respectively.

Currently, >20 bi-parental populations of sweet cherries are used for genetic mapping, including F_1 and a minimal number of F_2 populations. The population sizes range from 47 to 1386 individuals, with the largest population (1386) used for fine mapping [39]. The consensus genetic map, released concurrently with the first sweet cherry genome, holds the record for the highest number of markers (2382) in the sweet cherry genetic maps [22]. In contrast to the extensive mapping efforts in sweet cherry, genetic maps for non-sweet cherry species have generally featured a low number of individuals and genetic markers except Cai *et al.* [48], who developed a high-density consensus map for sour cherry by integrating independent maps from over five mapping populations, a total of 2058 markers covering 659.5 cM, which represents a mean marker interval of 0.3 cM.

Comparative analysis of this genetic map confirms, for the first time, a high level of chromosome synteny between sweet cherry and peach, providing evidence for a reciprocal application of genetic knowledge between peach and cherry. Most of these genetic maps and genetic markers have been collected and integrated into GDR. The high-quality and high-density linkage maps are still expected to be constructed for edible cherries, which could enhance the mapped QTL number as well as the precision.

QTL identification for varied traits

In the past 25 years, significant progress has been made in QTL mapping studies for various traits in edible cherries, with GDR already collecting >300 QTLs. Here, we review 94 highly reliable QTLs from sweet and sour cherries, as no QTLs have been reported on other edible cherries. The selection criteria include: (i) twice the natural log of Bayes factors ($2\ln\text{BF}$) >5 or logarithm of odds ratio (LOD) >3, (ii) percentage of variance explained (PVE) >5%, and (iii) detection in at least 2 years. With the exception of two studies [40, 49] reporting QTLs from a single year, Calle *et al.* [40] stand out as the only study focusing on precise phenotyping of chemical compounds related to fruit color by using high-performance liquid chromatography (HPLC) in edible cherries, which posed significant challenges in data collection. Despite the limitation of 1-year data, Rosyara *et al.* [49] identified powerful QTLs crucial for fruit size, including the well-known FW_G2a locus. The haplotype combinations of SSR markers BPPCT034 and CPST038, both located within the FW_G2a interval, have been confirmed as effective indicators for determining fruit size at the early stages [50].

Based on inputs from the cherry community, QTLs for 30 quantitative traits have been identified so far (Table 3). These traits were classified into four main categories: biochemical (including seven compounds related to anthocyanin biosynthesis), fruit

quality (encompassing traits related to fruit color, size, firmness, cracking, soluble solid content, and acidity), phenology (covering chilling requirement, flowering date, maturity date, and fruit development period), and physiology (focused on trunk diameter). The abbreviations and categories were proposed by referring to terms in the Plant Trait Ontology in GDR, with some modifications. In particular, we counted the number of years in which reliable QTLs were detected in single-year analysis (SY) or multi-year analysis (MY). Very stable QTLs across 10 years were reported for the flowering date (FD) [39].

Marker-trait association identified from GWAS

GWAS were reported on three sweet cherry germplasm collections covering >600 accessions: 116 from INRAE Prunus Genetic Resources Center at Bourran (Lot and Garonne, France) [35], 235 from the Research and Breeding Institute of Pomology Holovously Ltd [36], and 259 from Washington State University [51]. We reviewed 118 major GWAS loci from 17 traits with strong evidence: P -value <.05 and PVE > 3 (Table S1). They are classified into fruit quality, phenology, and physiology categories. Donkpegan *et al.* [35] used three reference genomes, one peach genome 'PLov2-2n' V2.0 and two sweet cherry genomes 'Regina' and 'Satonishiki', to conduct SNP-trait associations, Crump *et al.* [51] used *Prunus persica* var. 'PLov2-2n' V2.0, and Holušová *et al.* [36] used *P. avium* var. 'Tieton' V2.0. Regarding GWAS models, the performance of fixed and random model circulating probability unification (FarmCPU) was highlighted in datasets from Donkpegan *et al.* [35] and Holušová *et al.* [36]. Bayesian-information and linkage-disequilibrium iteratively nested keyway (Blink) and multi-locus mixed model (MLMM) were also employed by Crump *et al.* [51] and Donkpegan *et al.* [35], respectively. The use of multi-genome and multi-model strategy certainly strengthens the validity of the identified associations, and the consistent identification of major loci across these different models and genomes suggests a degree of convergence and reliability in the findings.

Genes conferring validated function

In general, the related traits display continuous phenotypic variation and are governed by multiple quantitative trait genes (QTGs), which can be identified by map-based cloning or GWAS [52]. Numerous candidate genes have been identified in the edible cherries' QTL intervals and upstream/downstream regions of the peak-associated loci. However, none of the QTGs have been functionally validated, and reverse genetic research is preferred to validate diverse biological and physiological functions of genes identified through comparative transcriptomic analysis. Also, they could serve as molecular keys to elucidate differences in traits, thus offering insights for genetic studies. Moreover, they could be explored for applications in molecular-assisted breeding (MAB) and molecular-assisted selection (MAS), and provide foundational information underlying molecular mechanisms.

As of June 2024, we have collected 48 genes cloned from edible cherries, including two genes from sour cherry (PcSOT1 and PcSOT2), four from Chinese cherry (CpARF7, CpCHS1, PpsGalAK-like, and PpsStv1), and 42 from sweet cherry (Table 4). These genes were classified into five categories and 15 sub-categories based on their involvement in a specific trait: abiotic stress (5 genes), biochemical (3 genes), fruit quality (24 genes), phenology (11 genes), and physiology (5 genes). The gene names are consistent with the nomenclature in the reference.

It is well known that the difficulty in functionally validating genes is a significant challenge in genetic transformation of stone fruit trees. However, *PavBBX6* and *PavBBX9* were successfully

Table 3. List of highly reliable QTLs in edible cherries (only reported in sweet cherry and sour cherry).

Category/sub-category (trait)	QTL label ¹	Label in GDR ²	Mapping population	Linkage group	QTL interval (cM)	QTL peak (cM)	LOD/2lnBF ³	PVE ³	Nb of years in SY/MY analysis ³	Reference
Biochemical										
Cyanidin 3-O-glucoside	q1_CY3G	qCYG.VC6 + 9-3.2	'Vic' × 'Cristobalina'	C3	41.9-59.45		3.1	11.9	SY: 1	[40]
	q2_CY3G	qCYG.VC6 + 9-3.1		V3	27.22-32.84		3.5	13.7	SY: 1	
Cyanidin 3-O-rutinoside	q3_CY3R	qCYR.VC6 + 9-3.2		C3	35.95-53.82		4.8	18.9	SY: 1	[40]
	q4_CY3R	qCYR.VC6 + 9-3.1		V3	20.39-31.56		5.5	22.7	SY: 1	
Neochlorogenic acid	q5_NeoChlorogenic acid	qNA.VC6 + 9-1.1		V1	141.34-142.9		19.9	60.3	SY: 1	[40]
	q6_NeoChlorogenic acid	qNA.VC6 + 9-3.1		V3	8.24-19.38		4	6.8	SY: 1	
p-Coumaric acid	q7_p-CA	qCA.VC6 + 9-1.1		V1	141.34-141.63		23.6	67.9	SY: 1	[40]
	p-Coumaroyl quinic acid	qCQA.VC6 + 9-1.1		V1	141.34-142.9		32.5	77.9	SY: 1	
Peonidin 3-O-glucoside	q9_Pe3G	qPEG.VC6 + 9-3.1		V3	19.39-31.53		3.6	16.4	SY: 1	[40]
Peonidin	q10_Pe3R	qPER.VC6 + 9-3.2		C3	45.17-48.39		5.3	21.8	SY: 1	
3-O-rutinoside	q11_Pe3R	qPER.VC6 + 9-4.1		C4	54.04-61.58		4.1	18.4	SY: 1	[40]
Fruit quality										
Fruit color (flesh)	q12_FC (flesh)	qFFC.VC6 + 9-3.2-2019	'Vic' × 'Cristobalina'	C3	32.47-82.33		12.3	32.2	SY: 1	[40]
	q13_FC (flesh)	qFFC.VC6 + 9-3.1-2019		V3	17.64-48		12.4	32.2	SY: 1	
Fruit color (skin)	q14_FC (flesh)		'New York 54' × 'Emperor Francis'	LG3		55.4	45.74	94.7	SY: 3	[103]
	q15_FC (skin)	qFSC.VC6 + 9-3.2-2018	'Vic' × 'Cristobalina'	C3	27.77-70.54		12.3	31.9	SY: 3	
Fruit cracking (fruit side)	q16_FC (skin)	qFSC.VC6 + 9-3.1-2018		V3	20.38-47.00		12.8	34.9	SY: 3	[40]
	q17_FC (skin)	qFSC.EN-ch3.2	'New York 54' × 'Emperor Francis'	LG3		54.2	27.8	86.8	SY: 3	
Fruit cracking (pistillar end)	q18_FC (skin)	qFSC.EN-ch3.2	Francis'	LG3		55.4	28	87.1	SY: 3	[51]
	q19_FCr	qFRCRK-LG1.1 multi	Multifamily	LG1	44-55	45	10.5	10.5	MY: 2/SY: 2	
Fruit cracking (fruit side)	q20_FCr	qFRCRK-LG5.1 multi		LG5	44-53	48		8.1	MY: 2/SY: 2	[45]
	q21_FCr (FS)		'Regina' × 'Garnet'	R2	2.1-8.9	5.5	37	15.2	MY: 7/SY: 2	
Fruit cracking (pistillar end)	q22_FCr (FS)		'Regina' × 'Lapins'	R2	11.8-76.7	47.6	37	15.2	MY: 7/SY: 2	[45]
	q23_FCr (FS)		'Regina' × 'Lapins'	L7	0-7.2	2.4	28.3	11.6	MY: 7/SY: 2	
Fruit cracking (pistillar end)	q24_FCr (FS)		'Regina' × 'Garnet'	L7	72.7-77.8	76.5	28.3	11.6	MY: 7/SY: 2	[45]
	q25_FCr (PE)		'Regina' × 'Garnet'	G4	15.3-26.3	20.8	29	13.7	MY: 7/SY: 2	
Fruit cracking (pistillar end)	q26_FCr (PE)		'Regina' × 'Lapins'	G4	79.5-95.2	93.9	29	13.7	MY: 7/SY: 2	[45]
	q27_FCr (PE)		'Regina' × 'Lapins'	R5	1.4-6.7	4	79.9	17.4	MY: 7/SY: 3	

(Continued)

Table 3. Continued

Category/sub-category (trait)	QTL label ¹	Label in GDR ²	Mapping population	Linkage group	QTL interval (cM)	QTL peak (cM)	LOD/2lnBF ³	PVE ³	Nb of years in SY/MY analysis ³	Reference
q28_FCr (PE)		'Regina' × 'Garnet'	R5	11.5–18.1	14.8	66.9	17.3	MY: 7/SY: 3		
q29_FCr (PE)		'Regina' × 'Lapins'	R5	34.7–39.4	37	79.9	17.4	MY: 7/SY: 3		
q30_FCr (PE)		'Regina' × 'Garnet'	R5	43.5–54	48.8	66.9	17.3	MY: 7/SY: 3		
Fruit cracking (stem end)	q31_FCr (SE)		'Fercer' × 'X'	X6	53.5–77.7	65.6	21.4	18.6	MY: 7/SY: 2	
	q32_FCr (SE)			X6	77.2–90.5	83.8	21.4	18.6	MY: 7/SY: 2	
Fruit firmness	q33_FF	qFRFRM-LG1.2 multi	Multifamily	LG1	34–70	48		21.8	MY: 3/SY: 3	[51]
	q34_FF	qFRFRM.A-ch1.1-Y1	'Ambrunés' × 'Sweetheart'	A1	60.30–76.29		4.08	18.8	SY: 2	[60]
	q35_FF	qFRFRM.S-ch1.2-Y1		S1	16.84–30.76		5	22.5	SY: 2	
	q36_FF	qFRFRM-LG3.2 multi	Multifamily	LG3	53–66	62		9.1	MY: 3/SY: 3	[51]
	q37_FF	qFRFRM-ch4.1 multi	Multifamily	LG4	50–54		11.7/9.5*	47.9/64.1	SY: 2	[42]
	q38_FF	qFRFRM.FX-X4.1	'Fercer' × 'X'	X4	33.1–36.0	34.5	125.3	70.2	MY: 7/SY: 7	[73]
	q39_FF	qFRFRM.FX-F4.1		F4	10.3–67.7	39	20.6	20.1	MY: 7/SY: 7	
	q40_FF		'Regina' × 'Garnet'	R5	13.9–67.7	44.7	25.5	24.1	MY: 4/SY: 4	[58]
	q41_FF			R5	67.7–67.7	67.7	25.5	24.1	MY: 4/SY: 4	
Fruit size	q42_FS	qFRSZ-ch2.1 multi	Multifamily	LG2	57–76		6.7/7.2*	23.6/21.5	SY: 2	[42]
	q43_FS (FLoD)		'New York 54' × 'Emperor Francis'	EF2		28.9	6	26	SY: 2	[59]
Fruit size (fruit longitudinal diameter)	q44_FS (FLoD)			NY2		41.4	7.7	19.4	SY: 2	
	q45_FS (FLoD)			NY6		56.8	11.2	37.8	SY: 2	
	q46_FS (FTD)			EF2		30.9	7.4	24.5	SY: 2	
Fruit size (fruit transverse diameter)	q47_FS (FTD)			NY2		44.4	7.3	26.1	SY: 2	
	q48_FS (FTD)			NY6		56.8	7.7	39.4	SY: 2	
Fruit size (fruit weight)	q49_FS (FW)	FRW.A-ch1.1-Y2	'Ambrunés' × 'Sweetheart'	A1	101.76–129.84		3.87	17.4	SY: 2	[60]
	q50_FS (FW)	qFRW/full-sib_families-LG1.	Four full-sib families	LG1		41	5.7*		SY: 1	[49]
	q51_FS (FW)	qFRW/full-sib_families-LG2.1		LG2		12.9	33.4*		SY: 1	
	q52_FS (FW)	qFRW/full-sib_families-LG2.2		LG2		20.9	33.4*		SY: 1	
	q53_FS (FW)	qFRW/full-sib_families-LG2.3		LG2		37	5.4*		SY: 1	

(Continued)

Table 3. Continued

Category/sub-category (trait)	QTL label ¹	Label in GDR ²	Mapping population	Linkage group	QTL interval (cM)	QTL peak (cM)	LOD/2lnBF ³	PVE ³	Nb of years in SY/MY analysis ³	Reference
q78_FD	qFD.RG-R4. multiyear	'Regina' × 'Garnet'	R4	18.4–22.5	20.4	76.1	36.3	MY: 5/SY: 5	[43]	
q79_FD		'Regina' × 'Garnet' pop1	R4	19–22.2	20.6	146.1	34.3	MY: 10/SY: 10	[39]	
q80_FD ^a	qBD.US-LG4.1	'Újfehértói Fürtös' × 'Surefire'	LG4	26.8–34.1	33.7	3.2		MY: 3	[48]	
q81_FD	qFD.RL-R4. multiyear	'Regina' × 'Lapins'	R4	27.9–31.2	29.6	47	21.2	MY: 6/SY: 6	[43]	
q82_FD		'Regina' × 'Lapins'	R4	33–34	33.2	57.2	47.2	MY: 4/SY: 4	[78]	
q83_FD ^a	qBD.M17x25-LG5.1	M172 × 25-02-29	LG5	11.6–34.4	25.7	3.5		MY: 3	[48]	
q84_FD		'Regina' × 'Garnet' pop1	R7	34.7–57.6	54.6	31.9	5.7	MY: 10/SY: 7	[39]	
Flowering date (beginning)	q85_FD (beginning)		'Regina' × 'Lapins'	L1	136.9–152.2	145.9	39.2	7.2	MY: 3–5 (ML: 5)	[76]
	q86_FD (beginning)			R4	0–0.5	29.4	149.6	20.9	MY: 3–5 (ML: 5)	
	q87_FD (beginning)			L6	8.6–23.4	16	42.2	7.3	MY: 3–5 (ML: 5)	
Fruit development period	q88_FDP	qFDT-ch4.2-multi	Multi-family	LG4	51–53		10.8/11.7*	65.3/64.5	SY: 2	[42]
Maturity date	q89_MD	qDMAT-ch2.1-multi		LG2	68–76		6.1/11.7*	11.7/10.4	SY: 2	
	q90_MD	qDMAT-ch4.2-multi		LG4	51–53		9.5/11.8*	46.8/52.5	SY: 2	
Physiology										
Trunk diameter	q91_TD	qTRDIA.WL-LG7.2012.2	'Wanhongzhu' × 'Lapins'	LG7		80.4	3.61	21.1	SY: 2	[90]
	q92_TD	qTRDIA.WL-LG7.2012.3		LG7		80.8	3.29	17.3	SY: 2	
	q93_TD	qTRDIA.WL-LG7.2012		LG7		78	3.24	15.7	SY: 2	
	q94_TD	qTRDIA.WL-LG8.2012		LG7		41.5	4.28	21.5	SY: 3	

Note: ¹ QTL label with ^a is detected from sour cherry, others are detected from sweet cherry; ² the names of QTLs included in the GDR; ³ highly reliable QTLs are with strong evidence (the two times the natural log of Bayes factors (2lnBF) > 5 or logarithm of odds ratio (LOD) > 3 and percentage of variance explained (PVE) > 5) over at least 2 years except for two studies ([40]; [49]) with QTLs from only 1 year. Calle et al. [40] is the sole study localizing chemical compounds in edible cherries, posing data collection challenges. Rosyara et al. [49] provide crucial insights into cherry genetics despite 1-year data; ³ the number of years/sites in which QTL was detected in single-year analysis (SY) or multi-year analysis (MY) in multi-sites (MS); * represent the data come from 2lnBF; -, data unavailable;

Table 4. List of experimentally validated genes in edible cherries.

Category/sub-category	Gene ¹	Chr	Position (Tieton V2.0) (Mb)	Function validated	Gene (protein) description	References
Abiotic stress						
Abiotic stress	<i>CpARF7^b</i>	7	26.34	Regulate drought and low phosphorus stress and root formation	Auxin response factor 7	[104]
Drought tolerance	<i>CpCHS1^b</i>	1	4.66	Enhance drought resistance	Chalcone synthase	[105]
Drought & salt tolerance	<i>PacCYP707A1</i>	5	17.69	Mediate drought tolerance	Abscisic acid 8'-hydroxylase 1-like	[85]
Drought & salt tolerance	<i>PaLectinL16</i>	4	14.96	Enhance resistance with abiotic (salt, drought) stresses	Lectin receptor-like kinases	[92]
Salt tolerance	<i>PaLectinL7</i>	2	40.05	enhance salt tolerance; promoted lignin deposition	lectin receptor-like kinases	[106]
Biochemical						
Fruit sorbitol and dry matter	<i>PcSOT1^a</i>	8	25.16	Regulate sorbitol and dry matter accumulation	Sorbitol transporter	[107]
matter	<i>PcSOT2^a</i>	8	25.18	Regulate sorbitol and dry matter accumulation	Sorbitol transporter	
Cherry allergy	<i>PaLTP</i>	6	33.34	Elicit cherry allergy (for Mediterranean population)	Non-specific lipid-transfer protein	[108]
Fruit quality						
Fruit color	<i>PavGST1</i>	3	5.11	Promote fruits' anthocyanin accumulation	Glutathione S-transferase F11-like	[70]
	<i>PacMYBA</i>	3	24.00	Promote anthocyanin accumulation in red-colored fruit	R2R3 MYB transcriptional regulator	[68]
	<i>PavMYB10.1</i>	3	24.00	Determine fruit colors	R2R3-MYB transcription factor MYB10.1 protein	[66]
	<i>PavBBX6</i>	3	30.30	Promote anthocyanin accumulation	B-box zinc finger protein 21-like	[53]
	<i>PavNCED1</i>	4	12.22	Promotes anthocyanin biosynthesis; promote ABA biosynthesis	9-cis-epoxycarotenoid dioxygenase NCED1	[(68); [54]]
	<i>PavBBX9</i>	4	12.71	Promote anthocyanin accumulation	B-box zinc finger protein 22	[53]
	<i>PacCOP1</i>	5	19.95	Negatively regulate anthocyanin biosynthesis	E3 ubiquitin-protein ligase COP1-like	[69]
Fruit cracking	<i>PaPIP1-4</i>	2	40.52	Prevent cracking by pre-harvest calcium treatments	Probable aquaporin PIP1-4	[75]
Fruit firmness (and rippen)	<i>PpsGalAK-like^b</i>	1	9.16	Increase protopectin content	Galacturonic acid-1-phosphate kinase	[31]
	<i>PavDof2</i>	1	44.39	Delay softening	Dof zinc finger protein DOF3.4	[54]
	<i>PavDof6</i>	2	44.31	Precocious, promote softening	Dof zinc finger protein DOF4.6-like	
	<i>PaMADS7</i>	3	32.12	Positively regulate fruit ripening and softening	MADS-box transcription factor	[(54); [74]]
	<i>PavARF8</i>	4	3.43	Delayed softening	Auxin response factor 3	[54]
	<i>PavPG38</i>	4	8.59	Reduce fruit firmness	Polygalacturonase	[71]
	<i>PavNAC56</i>	4	16.01	Promote ripening and softening	NAC transcription factor 25	[70]
	<i>PavDof15</i>	5	33.18	Delayed softening	Dof zinc finger protein DOF5.4	[54]
	<i>PavXTH14</i>	6	10.78	Reduce fruit firmness	Xyloglucan endotransglucosylase/hydrolase	[71]
	<i>PpsStw1^b</i>	6	13.13	Increase protopectin content	Homologous of glycosyltransferases 29 family	[31]
	<i>PavXTH15</i>	8	33.07	Reduce fruit firmness	Xyloglucan endotransglucosylase/hydrolase	[71]
Fruit size	<i>PavAGL15</i>	2	9.12	Increase fruit size	Agamous-like MADS-box protein AGL15	[62]
	<i>PacCYP78A9</i>	2	40.11	Increase fruit size	Cytochrome P450 78A9-like	[63]
	<i>PavRAV2</i>	3	31.27	Decrease fruit size (mesocarp cell expansion)	AP2/ERF and B3 domain-containing transcription repressor RAV2-like	[61]
	<i>PacCYP78A6</i>	5	28.23	Increase fruit size	Cytochrome P450 78A6-like	[64]
	<i>PavKLUH</i>	5	33.03	Increase fruit size (mesocarp cell expansion)	Pentatricopeptide repeat-containing protein PNM1	[61]

(Continued)

Table 4. Continued

Category/sub-category	Gene ¹	Chr	Position (Tieton V2.0) (Mb)	Function validated	Gene (protein) description	References
Phenology						
Flowering date (dormancy)	PavGA2ox-2 L	1	13.69	Delays flowering time, promote dwarf dense planting and inhibits seed germination	Gibberellin 2-beta-dioxygenase 2-like	[81]
	PavSEP	3	32.12	Shorten vegetative phase and promote early flowering	Developmental protein SEPALLATA 1	[82]
	PavNCEDES	4	5.42	Enhanced seed and flower bud dormancy	Probable 9-cis-epoxycarotenoid dioxygenase NCEDES	[84]
	PavCIG1	5	25.25	Delayed flowering	Dehydration-responsive element-binding protein 1E-like	[87]
	PavCIG2	5	25.26	Repress flowering and maintain the dormancy status	Dehydration-responsive element-binding protein 1E	
	PavFUL	5	33.10	Led to early flowering and multi-silique formation	Truncated transcription factor CAULIFLOWER A	[83]
	PavTCP17	5	33.53	Positively regulate flower bud dormancy	Hypothetical protein	[86]
	PavSVP	6	26.16	Maintain suppression phase of flowering	MADS-box protein SVP	[82]
	PavFT	6	37.56	promote flowering	protein HEADING DATE 3A	[109]
Maturity date	PacCYP707A2	7	22.51	Negatively regulate cherry fruit ripening	Abscisic acid 8'-hydroxylase 4-like	[85]
Physiology						
Flower and seed	PavDAM1	1	54.64	Result in abnormal flower and seed development	MADS-box protein JOINTLESS-like	[80]
	PavDAM5	1	54.70	Result in abnormal flower and seed development	MADS-box protein JOINTLESS-like	
Plant hormone signaling	PavSOC1	2	33.89	Result in abnormal flower and seed development	MADS-box protein SOC1	[80]
	PavNRT2.1	6	10.53	Regulate nitrate signaling pathways	High-affinity nitrate transporter 2.1-like	[91]
Self-incompatibility	PaLAX1	6	31.72	Promote cell uptake of auxin	Auxin transporter-like protein 2	[110]
	S4-SLFL2	6	34.99	Mediate the ubiquitination and degradation of S-RNase	S locus F-box protein	[89]

Note: Genes with multiple function are categorized into the first appearing category based on the order of function validated; ¹ genes with ^a are cloned from sour cherry, genes with ^b are validated in Chinese cherry, others are cloned from sweet cherry.

overexpressed in sweet cherry calli to enhance light-induced anthocyanin biosynthesis and abscisic acid (ABA) accumulation [53]. Many genes, like *PavDof2/6/15*, *PavNAC56*, *PpsGalAK*-like, and *PpsStv1* were successfully transiently overexpressed in sweet cherry fruit [31, 54].

Genetic architecture of traits by integrating QTLs, GWAS loci, and functional genes

Genetic architecture refers to the characteristics of genetic variation that drive heritable phenotypic variability. It is influenced by the number of genetic variants affecting a trait, population frequencies, the magnitude of their effects, and their interactions with each other and the environment [55]. Understanding the genetic architecture of complex traits is a central goal of cherry genetics research. Here, we drew a comprehensive genetic architecture detailing the traits of edible cherries by integrating QTLs, GWAS loci, and functional genes into the reference genome *P. avium* 'Tieton' V2.0 (Fig. 1, Table S2).

The highly reliable QTLs originate from genetic maps with varying resolutions as well as GWAS data spanning across different genomes. This fragmentation of genetic information across various sources hampers our ability to comprehensively analyze and understand complex trait architectures. To overcome this challenge, we conducted a genome-wide alignment to the *P. avium* 'Tieton' V2.0 genome by using BLAST on GDR (<https://www.rosaceae.org/blast/nucleotide/nucleotide>) with default parameters. For QTLs, the physical positions were predominantly determined by aligning marker sequences at both ends of the QTL interval. For GWAS loci, sequences within 1000 bp upstream and downstream to the peak SNP were extracted for alignment. TBtools-II [56] was employed for extracting sequences. Validity was assessed based on an identity percentage >90% for all alignment entries; if not met, sequences within 2000 bp upstream and downstream were utilized. For functional genes, coding sequences or primer sequences were used for alignment. This work will lead to enhanced genetic resources, thereby accelerating genetic discovery for cherry improvement.

Fruit size and fruit weight

The size and weight of cherry fruits are crucial factors determining their overall quality and appeal to consumers, often described using terms like longitude (length), transverse (diameter/width), and lateral diameter (thickness), etc. This dimensionality largely depends on a coordinated series of cell divisions and expansions in the fleshy mesocarp [57]. We reviewed 26 reported QTLs underlying fruit size and weight across chromosomes 1, 2, 3, and 6. Among these 26 QTLs, 17 (*q42*, *q43*, *q44*, *q46*, *q47*, *q51* to *q57*, and *q60* to *q65*) were co-localizing in a narrow interval on Chr2, including peak markers BPPCT034 and CSPSCT038 [49, 58, 59]. Moreover, Holušová et al. [36] confirmed five fruit size-related GWAS SNPs (*g57*, *g64*, *g65*, *g74*, *g89* in Fig. 1 and Table S2) positioned around 29 Mb on Chr2, within the 'hot' QTL interval of fruit size, exhibiting strong associations ($p < 1.0 \times 10^{-10}$). Hence, new QTL or GWAS was discovered near the 'hot' interval; it draws the attention of breeders and geneticists. Additionally, two fruit weight QTLs, *q50_FS* (FW) [60] and *q49_FS* (FW) [49], share an overlapping region of ~1.8 Mb on Chr1. Pit size-related QTLs (*q66_FS* (PTrD) and *q67_FS* (PLoD)) on Chr6 were located at the same position as QTLs for fruit diameter (*q45_FS* (FLoD) and *q48_FS* (FTrD)) and fruit size QTL *q60_FS* (FW) [59]. The strong genetic linkage between fruit size and pit size highlights the potential difficulty in implementing an effective

genetic improvement strategy that would involve the increasing of flesh area while simultaneously decreasing the pit size. Notably, five genes were confirmed to regulate sweet cherry fruit size through virus-induced gene silencing. *PavRAV2* [61] and *PavAGL15* [62] are negative regulators, and they suppressed fruit enlargement by weakening mesocarp cell expansion and cell cycling and proliferation, respectively. *PaCYP78A9* is likely to be an important upstream regulator of cell cycle processes and *PaCYP78A6* acts redundantly with *PaCYP78A9* to affect fruit size [63, 64]. Silencing *PavRAV2* resulted in enlarged fruit due to enhanced mesocarp cell expansion. More precisely, the mesocarp cell length and volume in the *PavRAV2*-silenced sweet cherry fruits increased by 58% and 26%, respectively, compared with those of the control fruits [61]. Significantly, we observed that *PavRAV2* is located within the QTL *q58_FS* (FW), which has a large additive effect (~1.6 g) on fruit size [49]. This suggests that further in-depth investigation of gene *PavRAV2* could be crucial for explaining the genetic variation in fruit size. Besides, silencing *PavKLUH* resulted in decreased fruit size by restricting mesocarp cell expansion [61].

Fruit color

Edible cherry fruits exhibit a range of rich colors from white to black purple, directly influencing their commercial value. By compiling previously reported results, Chr3 plays a crucial role in controlling cherry fruit color, housing six GWAS loci, seven QTLs, and four validated genes related to flesh or skin color, and fruit coloration in edible cherries results from anthocyanin accumulation [11, 65]. The QTLs for essential metabolites regulating anthocyanin biosynthesis pathway are also located on Chr3 [40] (Fig. 1, Table S2). All fruit color QTLs on LG3 shared a common 6.43-Mb interval (from the top of *q14/17/18* to the bottom of *q15*). As expected, the R2R3 MYB transcription factor *PavMYB10.1* is located in this region, which has been confirmed as the major determinant in anthocyanin biosynthesis. Three different alleles, *PavMYB10.1c*, *PavMYB10.1b*, and *PavMYB10.1a*, determine yellow, blush, and dark-red colors, respectively. Color segregation in two F₁ populations conforms to Mendel first segregation law in a 3:1 ratio and a 1:1 ratio, revealing that *PavMYB10.1a* was dominant to *PavMYB10.1b* [66]. Metabolomic profiling of cherries has demonstrated that cyanidins play a dominant role in fruit color determination [11, 67]. Notably, *PavMYB10.1* is also located in three QTLs for cyanidins (*q3_CY3R*, *q4_CY3R* and *q1_CY3G*) [40]. Therefore, it can be inferred more precisely that *PavMYB10.1* determines cherry color by modulating cyanidin synthesis in the anthocyanin biosynthesis pathway, thus providing insights into refining the regulatory network and genetic mechanisms underlying cherry color.

Another noteworthy location for regulating cherry color is the middle of Chr4, where two validated genes (*PavNCED1* and *PavBBX9*) [68, 53, 54] were identified within the 2 Mb interval upstream of the QTL for peonidin 3-O-rutinoside [40] (*q11_Pe3R*: 14.17–16.76 Mb) (Table S2). *PavNCED1* is an important gene in the ABA biosynthesis pathway, with its expression promoted by *PavBBX6* and *PavBBX9*, which together positively regulate light-induced anthocyanin accumulation [53]. Therefore, peonidin 3-O-rutinoside, capable of imparting a deep red or purple color to the fruit, is speculated to be the specific anthocyanin compound regulated by *PavNCED1* and *PavBBX9*. Several other genes have been confirmed to participate in color formation. *PacCOPI1* negatively regulates anthocyanin biosynthesis, while *PavGST1* positively regulates sweet cherry fruit anthocyanin accumulation, with its transcription being activated by *PavMYB10.1* [70, 69].

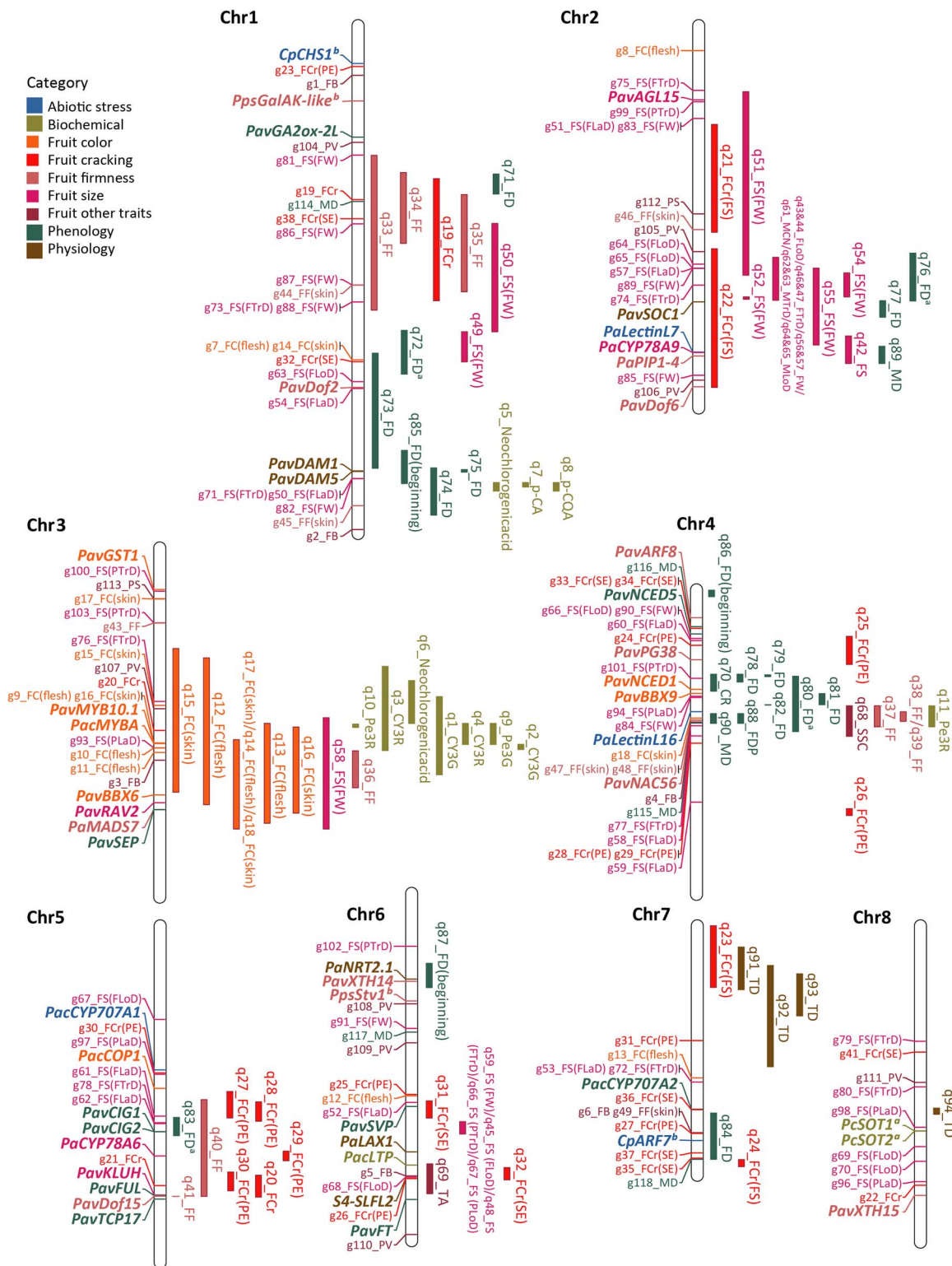


Figure 1. Genetic architecture of traits by integrating QTLs (Table 3), GWAS loci (Table S1) and functional genes (Table 4) into the reference genome ‘Tieton’ V2.0. On the right side of the chromosome, each QTL delimits an approximate physical range based on LOD support intervals of QTL identified from different studies. GWAS loci and functional genes are present to the left of the chromosome, and the functional genes are in bold italics. Detailed information is available in Table S2.

Fruit cracking and firmness

Cracking is the most severe abiotic threat to profitability in sweet cherries, and high firmness ensures post-harvest quality and adequate shelf life. Among sweet cherry fruit quality traits, firmness has been rated third in importance by consumers, above

size and color (Zheng et al., 2016). These processes are modulated by a set of cell wall-modifying enzymes, the most studied of which include xyloglucan endotransglucosylase/hydrolases (XTHs) and polygalacturonases (PGs). Genetic architecture of fruit cracking and firmness is complex, with QTLs and GWAS loci widely

distributed across seven chromosomes except the eighth chromosome. Among 18 *PavXTHs* and 45 *PavPGs*, *PavXTH14*, *PavXTH15*, and *PavPG38* significantly reduce the fruit firmness through modification of pectin and hemicellulose [71]. MADS-box genes constitute a highly conserved family of transcription factors and are involved in floral organogenesis, flowering time, embryo and fruit development, and ripening. Qi et al., [72] revealed that *PaMADS7* binds to the promoter of *PaPG1*, serving as an indispensable positive regulator of sweet cherry fruit ripening and softening.

On Chr4, a validated NAC transcription factor (*PavNAC56*) is located in three highly reliable QTLs for firmness (*q37_FF*, *q38_FF*, and *q39_FF*), with *q38_FF* being particularly noteworthy as it was identified in MY and SY analysis for 7 years with maximum LOD of 125 and PVE of 75% [73, 42]. *PavNAC56* plays an indispensable role in controlling the ripening and softening of sweet cherry fruit. It directly binds to the promoters of several genes related to cell wall metabolism (*PavPG2*, *PavEXPA4*, *PavPL18*, and *PavCEL8*) and activates their expression [74]. On Chr 2, *PaPIP1;4*, together with *PavDof6*, is located within the *q22_FCr(FS)* interval. *PaPIP1;4* is the only plasma membrane aquaporin validated to prevent cherry fruit cracking, which is upregulated by pre-harvest calcium treatment [75]. ABA-responsive transcription factor *PavDof6* results in precocious ripening of sweet cherry fruit. Along with *PavDof2/15*, *PavDof6* is activated by auxin response factor *PavARF8*, and they all directly bind to the *PavNCED1* promoter and regulate its expression, forming a feedback mechanism for ABA-mediated cherry fruit softening [54]. *PavDof15*, located on Chr5, has the same function as *Pavdof2* in delaying cherry fruit softening, and it is also located within the interval of firmness and cracking-related QTLs (*q40_FF*, *q20_FCr*, and *q41_FF*). On LG1, there are four QTLs related to firmness and cracking (*q33_FF*, *q34_FF*, *q19_FCr*, *q35_FF*), sharing a notable 5.99-Mb overlap interval. Within this region lies an SNP, *g19_FCr*, which exhibits a high PVE of 12.7% [51], underscoring its considerable potential for further exploration.

Phenology

Phenology traits and their findings will enable increased efficiency of breeding strategies focused on adaptation to future climatic conditions. Phenology traits like FD and maturity date were reported to be highly polygenic, and many QTLs with high PVE values were identified [44]. The end of Chr1 and the middle of Chr4 are identified as two 'hotspot' regions where FD QTLs from both sweet cherry and sour cherry aggregate, according to previous studies [43, 77, 39, 48, 42, 78, 76] (Fig. 1, Table S2). However, within these two 'hotspot' QTL intervals, no GWAS loci neither validated genes have been reported yet. Particularly, MADS-box transcription factors have been identified as strong candidate genes for the genetic control of blooming and temperature responses in many species, with structural mutations in *PavDAMs* validated as a DNA-based marker for selection [79]. However, in sweet cherry, functional and expression analyses of *PavDAM1/5* showed that they might have a role in flower development instead of endodormancy induction and bud formation [80].

Nevertheless, there are still 11 functional genes related to phenology distributed on the first seven chromosomes. *PavGA2ox-2 L* functions as a GA metabolic gene that promotes dwarf dense planting, delays flowering time, and inhibits seed germination [81]. The overexpression of *PavSEP* and *PavFUL* in *Arabidopsis* leads to early flowering promotion [82, 83], and *PavNCED5* promoted flower bud dormancy [84]. The negative regulator *PacCYP707A2* and positive regulator *PavTCP17* are both involved in regulating ABA synthesis, but act on bud dormancy and fruit ripening in sweet cherry, respectively [85, 86]. C-repeat binding factor (CBF)

plays an important role in response to low temperature. Two novel CBF homologous genes of sweet cherry, *PavCIG1* and *PavCIG2*, were isolated with the function of repressing flowering, falling within the narrow *q83_FD* (~2.2 Mb) interval on Chr5 [48, 87]. *PavFT* is expressed during floral bud determination and can promote flowering in a winter-annual *Arabidopsis* accession [83]. The MADS-box transcription factor *PavSVP* exhibits the functions in maintaining the suppression phase of flowering [82].

Physiological and abiotic stress traits

Self-incompatibility (SI) of cherry species is genetically controlled by a single polymorphic S locus, which harbors a single S-RNase as the pistil S determinant and several F-box genes as pollen S determinants ([21]; Matsumoto et al., 2012). Moreover, the insertion of the putative M locus-encoded GST (MGST) promoter region also probably leads to the SC in the cultivar 'Cristobalina' despite lacking functional validation [88]. Precisely, *S4-SLFL2* plays a role in mediating the ubiquitination and degradation of S-RNase, leading to SC in the cultivar 'Lapins' [89].

Trunk diameter (TD) is a physiological trait correlated with tree vigor, resistance, and fruit yield. Four QTLs on Chr7 and Chr8 provide genetic information for controlling this trait [90]. *PaNRT2.1* mediates dark septate endophyte (DSE)-dependent nitrogen assimilation in sweet cherry roots [91].

Several genes for abiotic stress traits have been validated through reverse genetics, including two cloned from Chinese cherry: *CpCHS1* increases drought tolerance (Hou et al., 2022), and *CpARF7* responds to drought tolerance and low phosphorus (Hou et al., 2022). *PaLectinL16* enhances sweet cherry resistance with salt stress [92], and so on (Table 4). Overall, all these studies demonstrate that any issue affecting cherry growth, development, productivity, and geographic adaptation is one that needs to be addressed.

Concluding remarks and prospects

We summarized the current progress in edible cherries genomes and genomics, focusing on genetic maps, QTLs, GWAS loci, and validated functional genes. By integrating these genetic findings into the 'Tieton' V2.0 genome, a global genetic architecture of main agronomic traits was established, which could be served as a reference for further advancements in edible cherries. However, species-specific challenges remain. Current research mainly focused on diploid sweet cherries, particularly on fruit quality and phenological traits. However, enhancing abiotic stress tolerance is a pressing challenge in the context of global climate change. The complex tetraploid genomes of sour cherry and Chinese cherry have slowed genetic progress, yet their recent genome sequences offer opportunities to address limitations like small fruit size, soft texture, and short shelf life. Genetic studies on Nanking cherry (*P. tomentosa*) remain limited, but its unique shrub form and the medicinal properties of its seeds [93] provide promising avenues for future exploration.

Alongside the increasing availability of genomic resources and growing analytical approaches such as multi-omics, it will be possible to pinpoint the genomic regions, the genes, and the molecular mechanisms involved in the genetic determinism of traits of interest in edible cherries. Moreover, the genomic transferability among *Prunus* species leads this review to a possible broader application. Insights obtained about a gene associated with a specific trait in one edible cherry species can be extrapolated to another species within the genus, facilitating the exploration of similar traits across different species. The co-localizations

integrated in this review will enable researchers to undertake comparative studies more efficiently, thereby accelerating the transfer of knowledge and breeding innovations across *Prunus* species. Finally, the availability of sequence data and targeted genomic regions involved in the variation of a trait will allow the construction of an interspecific pangenome of edible cherries, and a pangenome will make it possible to identify common genomic regions under selection pressure in common between the species. The 'hot' regions for specific traits could ultimately guide cherry breeding strategies and genetic improvement programs.

Acknowledgement

This work was financially supported by Sichuan Science and Technology Program (2024YFHZ0302), Natural Science Foundation of Sichuan Province (2023NSFSC0158), Sichuan Fruit Innovation Team of National Modern Agricultural Industrial Technology System in China (SCCXTD-2024-4), the Project of Rural Revitalization Research Institute in Tianfu New Area of Sichuan Province (XZY1-04) and Cherry Resources Sharing and Service Platform of Sichuan Province.

Author contributions

Z.-S.L. collected and analyzed data and wrote the manuscript; A.B. and E.D. collected data and conceived and revised the manuscript; W.Y. revised the manuscript; and X.-R.W. supervised and revised the manuscript.

Data availability

All the data is presented in the text file.

Conflict of interest

The authors declare no conflict of interests.

Supplementary Data

Supplementary data is available at Horticulture Research online.

References

- Liu Z, Ma H, Jung S. et al. Developmental mechanisms of fleshy fruit diversity in Rosaceae. *Annu Rev Plant Biol.* 2020a;**71**:547–73
- Cao J, Jiang Q, Lin J. et al. Physicochemical characterisation of four cherry species (*Prunus* spp.) grown in China. *Food Chem.* 2015;**173**:855–63
- Quero-García J, Iezzoni A, Puławska J. et al. *Cherries: Botany, Production and Uses*. Boston, MA: CABI International, 2017
- Wang L, Feng Y, Wang Y. et al. Accurate chromosome identification in the *Prunus* subgenus *Cerasus* (*Prunus pseudocerasus*) and its relatives by oligo-FISH. *Int J Mol Sci.* 2022;**23**:13213
- Karagiannis E, Sarrou E, Michailidis M. et al. Fruit quality trait discovery and metabolic profiling in sweet cherry genebank collection in Greece. *Food Chem.* 2020;**342**:128315
- Mansoori S, Dini A, Chai SC. Effects of tart cherry and its metabolites on aging and inflammatory conditions: efficacy and possible mechanisms. *Ageing Res Rev.* 2021;**66**:101254
- Dirlwanger E, Claverie J, Iezzoni A. et al. Sweet and sour cherries: linkage maps, QTL detection and marker assisted selection. In: Folta KM, Gardiner SE (eds.), *Genetics and Genomics of Rosaceae*. New York, NY: Springer, 2009,291–313
- Faust M, Surányi D. Origin and dissemination of cherry. *Hortic Rev.* 1997;**19**:263–317
- Chen T, Li L, Zhang J. et al. Investigation, collection and preliminary evaluation of genetic resources of Chinese cherry [*Cerasus pseudocerasus* (Lindl.) G. Don]. *J Fruit Sci.* 2016;**33**:917–33
- Wang Y, Hu G, Liu Z. et al. Phenotyping in flower and main fruit traits of Chinese cherry [*Cerasus pseudocerasus* (Lindl.) G. Don]. *Sci Hortic.* 2022b;**296**:110920
- Liu Z, Wang H, Zhang J. et al. Comparative metabolomics profiling highlights unique color variation and bitter taste formation of Chinese cherry fruits. *Food Chem.* 2024;**439**:138072
- Zhang Q, Yan G, Dai H. et al. Characterization of Tomentosa cherry (*Prunus tomentosa* Thunb.) genotypes using SSR markers and morphological traits. *Sci Hortic.* 2008;**118**:39–47
- Choi C, Kappel F. Inbreeding, coancestry, and founding clones of sweet cherries from North America. *J Am Soc Hortic Sci.* 2004;**129**:535–43
- Duan X, Li M, Yue T. et al. Fruit scientific research in new China in the past 70 years: cherry. *J Fruit Sci.* 2019;**36**:1339–51
- Sansavini S, Lugli S. Sweet cherry breeding programs in Europe and Asia. *Acta Hortic.* 2008;41–58
- Quero-García J, Branchereau C, Barreneche T. et al. DNA-informed breeding in sweet cherry: current advances and perspectives. *Italus Hortus.* 2022;**29**:14
- Liu J, Li M, Zhang Q. et al. Exploring the molecular basis of heterosis for plant breeding. *J Integr Plant Biol.* 2020b;**62**:287–98
- Paril J, Reif J, Fournier Level A. et al. Heterosis in crop improvement. *Plant J.* 2024;**117**:23–32
- Aranzana MJ, Decroocq V, Dirlwanger E. et al. *Prunus* genetics and applications after de novo genome sequencing: achievements and prospects. *Hortic Res.* 2019;**6**:58
- Jung S, Lee T, Cheng C. et al. 15 years of GDR: new data and functionality in the genome database for Rosaceae. *Nucleic Acids Res.* 2019;**47**:D1137–45
- Akagi T, Henry IM, Morimoto T. et al. Insights into the *Prunus*-specific S-RNase-based self-incompatibility system from a genome-wide analysis of the evolutionary radiation of S locus-related F-box genes. *Plant Cell Physiol.* 2016;**57**:1281–94
- Shirasawa K, Isuzugawa K, Ikenaga M. et al. The genome sequence of sweet cherry (*Prunus avium*) for use in genomics-assisted breeding. *DNA Res.* 2017;**24**:499–508
- Wang J, Liu W, Zhu D. et al. Chromosome-scale genome assembly of sweet cherry (*Prunus avium* L.) cv. Tieton obtained using long-read and Hi-C sequencing. *Hortic Res.* 2020a;**7**:122
- Wang J, Liu W, Zhu D. et al. A de novo assembly of the sweet cherry (*Prunus avium* cv. Tieton) genome using linked-read sequencing technology. *PeerJ.* 2020b;**8**:e9114
- Le Dantec L, Girollet N, Jérôme G. et al. *Assembly and Annotation of 'Regina' Sweet Cherry Genome (Recherche Data Gouv, V1)*. 2020. <https://doi.org/10.15454/KEW474>.
- Pinosio S, Marroni F, Zuccolo A. et al. A draft genome of sweet cherry (*Prunus avium* L.) reveals genome-wide and local effects of domestication. *Plant J.* 2020;**103**:1420–32
- Zhang X, Duan X, Wang J. et al. Insights into the evolution and fruit color change-related genes of chromosome doubled sweet cherry from an updated complete T2T genome assembly. *iMetaOmics.* 2024;**2024**:e13
- Olden EJ, Nybom N. On the origin of *Prunus cerasus* L. *Hereditas.* 1968;**59**:327–45
- Tavaud M, Zanetto A, David JL. et al. Genetic relationships between diploid and allotetraploid cherry species (*Prunus*

- avium*, *Prunus x gondouinii* and *Prunus cerasus*). *Heredity (Edinb)*. 2004;**93**:631–8
30. Goeckeritz CZ, Rhoades KE, Childs KL. et al. Genome of tetraploid sour cherry (*Prunus cerasus* L.) 'Montmorency' identifies three distinct ancestral *Prunus* genomes. *Hortic Res*. 2023;**10**:d97
 31. Jiu S, Lv Z, Liu M. et al. Haplotype-resolved genome assembly for tetraploid Chinese cherry (*Prunus pseudocerasus*) offers insights into fruit firmness. *Hortic Res*. 2024;uhae142
 32. Wang Y, Li X, Feng Y. et al. Autotetraploid origin of Chinese cherry revealed by chromosomal karyotype and in situ hybridization of seedling progenies. *Plants (Basel)*. 2023a;**12**:3116
 33. Peace C, Bassil N, Main D. et al. Development and evaluation of a genome-wide 6K SNP array for diploid sweet cherry and tetraploid sour cherry. *PLoS One*. 2012;**7**:e48305
 34. Vanderzande S, Zheng P, Cai L. et al. The cherry 6+9K SNP array: a cost-effective improvement to the cherry 6K SNP array for genetic studies. *Sci Rep*. 2020;**10**:7613
 35. Donkpegan ASL, Bernard A, Barreneche T. et al. Genome-wide association mapping in a sweet cherry germplasm collection (*Prunus avium* L.) reveals candidate genes for fruit quality traits. *Hortic Res*. 2023;**10**:d191
 36. Holušová K, Čmejlová J, Suran P. et al. High-resolution genome-wide association study of a large Czech collection of sweet cherry (*Prunus avium* L.) on fruit maturity and quality traits. *Hortic Res*. 2023;**10**:c233
 37. Liu Z, Zhang J, Wang Y. et al. Development and cross-species transferability of novel genomic-SSR markers and their utility in hybrid identification and trait association analysis in Chinese cherry. *Horticulturae*. 2022;**8**:222
 38. Xanthopoulou A, Manioudaki M, Bazakos C. et al. Whole genome re-sequencing of sweet cherry (*Prunus avium* L.) yields insights into genomic diversity of a fruit species. *Hortic Res*. 2020;**7**:60
 39. Branchereau C, Quero-García J, Zaracho-Echagüe NH. et al. New insights into flowering date in *Prunus*: fine mapping of a major QTL in sweet cherry. *Hortic Res*. 2022;**9**:c42
 40. Calle A, Serradilla MJ, Wunsch A. QTL mapping of phenolic compounds and fruit colour in sweet cherry using a 6+9K SNP array genetic map. *Sci Hortic*. 2021a;**280**:109900
 41. Calle A, Cai L, Iezzoni A. et al. High-density linkage maps constructed in sweet cherry (*Prunus avium* L.) using cross- and self-pollination populations reveal chromosomal homozygosity in inbred families and non-syntenic regions with the peach genome. *Tree Genet Genomes*. 2018;**14**:37
 42. Calle A, Wunsch A. Multiple-population QTL mapping of maturity and fruit-quality traits reveals LG4 region as a breeding target in sweet cherry (*Prunus avium* L.). *Hortic Res*. 2020;**7**:127
 43. Castede S, Campoy JA, Garcia JQ. et al. Genetic determinism of phenological traits highly affected by climate change in *Prunus avium*: flowering date dissected into chilling and heat requirements. *New Phytol*. 2014;**202**:703–15
 44. Hardner CM, Hayes BJ, Kumar S. et al. Prediction of genetic value for sweet cherry fruit maturity among environments using a 6K SNP array. *Hortic Res*. 2019;**6**:6–15
 45. Quero-García J, Letourmy P, Campoy JA. et al. Multi-year analyses on three populations reveal the first stable QTLs for tolerance to rain-induced fruit cracking in sweet cherry (*Prunus avium* L.). *Hortic Res*. 2021;**8**:136
 46. Stockinger EJ, Mulinix CA, Long CM. et al. A linkage map of sweet cherry based on RAPD analysis of a microspore-derived callus culture population. *J Hered*. 1996;**87**:214–8
 47. Klagges C, Campoy JA, Quero-García J. et al. Construction and comparative analyses of highly dense linkage maps of two sweet cherry intra-specific progenies of commercial cultivars. *PLoS One*. 2013;**8**:e54743
 48. Cai L, Stegmeir T, Sebolt A. et al. Identification of bloom date QTLs and haplotype analysis in tetraploid sour cherry (*Prunus cerasus*). *Tree Genet Genomes*. 2018;**14**:22
 49. Rosyara UR, Bink MCAM, van de Weg E. et al. Fruit size QTL identification and the prediction of parental QTL genotypes and breeding values in multiple pedigreed populations of sweet cherry. *Mol Breeding*. 2013;**32**:875–87
 50. Szilágyi S, Horváth-Kupi T, Desiderio F. et al. Evaluation of sweet cherry (*Prunus avium* L.) cultivars for fruit size by FW_G2a QTL analysis and phenotypic characterization. *Sci Hortic*. 2022;**292**:110656
 51. Crump WW, Peace C, Zhang Z. et al. Detection of breeding-relevant fruit cracking and fruit firmness quantitative trait loci in sweet cherry via pedigree-based and genome-wide association approaches. *Front Plant Sci*. 2022;**13**:823250
 52. Huang X, Huang S, Han B. et al. The integrated genomics of crop domestication and breeding. *Cell*. 2022;**185**:2828–39
 53. Wang Y, Xiao Y, Sun Y. et al. Two B-box proteins, *PavBBX6/9*, positively regulate light-induced anthocyanin accumulation in sweet cherry. *Plant Physiol*. 2023b;**192**:2030–48
 54. Zhai Z, Xiao Y, Wang Y. et al. Abscisic acid-responsive transcription factors *PavDof2/6/15* mediate fruit softening in sweet cherry. *Plant Physiol*. 2022;**190**:2501–18
 55. Timpson NJ, Greenwood C, Soranzo N. et al. Genetic architecture: the shape of the genetic contribution to human traits and disease. *Nat Rev Genet*. 2018;**19**:110–24
 56. Chen C, Wu Y, Li J. et al. TBtools-II: a “one for all, all for one” bioinformatics platform for biological big-data mining. *Mol Plant*. 2023;**16**:1733–42
 57. Olmstead JW, Iezzoni AF, Whiting MD. Genotypic differences in sweet cherry fruit size are primarily a function of cell number. *J Am Soc Hortic Sci*. 2007;**132**:697–703
 58. Campoy JA, Le Dantec L, Barreneche T. et al. New insights into fruit firmness and weight control in sweet cherry. *Plant Mol Biol Report*. 2015;**33**:783–96
 59. Zhang G, Sebolt AM, Sooriyapathirana SS. et al. Fruit size QTL analysis of an F₁ population derived from a cross between a domesticated sweet cherry cultivar and a wild forest sweet cherry. *Tree Genet Genomes*. 2010;**6**:25–36
 60. Calle A, Balas F, Cai L. et al. Fruit size and firmness QTL alleles of breeding interest identified in a sweet cherry 'Ambrunés' × 'Sweetheart' population. *Mol Breeding*. 2020a;**40**:86
 61. Qi X, Liu L, Liu C. et al. Sweet cherry AP2/ERF transcription factor, *PavRAV2*, negatively modulates fruit size by directly repressing *PavKLUH* expression. *Physiol Plant*. 2023;**175**:14065
 62. Dong Y, Qi X, Liu C. et al. A sweet cherry AGAMOUS-LIKE transcription factor *PavAGL15* affects fruit size by directly repressing the *PavCYP78A9* expression. *Sci Hortic*. 2022;**297**:110947
 63. Qi X, Liu C, Song L. et al. *PaCYP78A9*, a cytochrome P450, regulates fruit size in sweet cherry (*Prunus avium* L.). *Front Plant Sci*. 2017;**8**:2076
 64. Qi X, Liu C, Song L. et al. *Arabidopsis* EOD3 homologue *PaCYP78A6* affects fruit size and is involved in sweet cherry (*Prunus avium* L.) fruit ripening. *Sci Hortic*. 2019;**246**:57–67
 65. Sun L, Huo J, Liu J. et al. Anthocyanins distribution, transcriptional regulation, epigenetic and post-translational modification in fruits. *Food Chem*. 2023;**411**:135540

66. Jin W, Wang H, Li M. et al. The R2R3MYB transcription factor *PavMYB10.1* involves in anthocyanin biosynthesis and determines fruit skin colour in sweet cherry (*Prunus avium* L.). *Plant Biotechnol J.* 2016;**14**:2120–33
67. Wang Y, Wang Z, Zhang J. et al. Integrated transcriptome and metabolome analyses provide insights into the coloring mechanism of dark-red and yellow fruits in Chinese cherry [*Cerasus pseudocerasus* (Lindl.) G. Don]. *Int J Mol Sci.* 2023c;**24**:3471
68. Shen X, Zhao K, Liu L. et al. A role for *PacMYBA* in ABA-regulated anthocyanin biosynthesis in red-colored sweet cherry cv. Hong Deng (*Prunus avium* L.). *Plant Cell Physiol.* 2014;**55**:862–80
69. Liang D, Zhu T, Deng Q. et al. *PacCOP1* negatively regulates anthocyanin biosynthesis in sweet cherry (*Prunus avium* L.). *J Photochem Photobiol B Biol.* 2020;**203**:111779
70. Qi X, Liu C, Song L. et al. A sweet cherry glutathione S-transferase gene, *PavGST1*, plays a central role in fruit skin coloration. *Cells.* 2022;**11**:1170
71. Zhai Z, Feng C, Wang Y. et al. Genome-wide identification of the *Xyloglucan endotransglucosylase/hydrolase (XTH)* and *Polygalacturonase (PG)* genes and characterization of their role in fruit softening of sweet cherry. *Int J Mol Sci.* 2021;**22**:12331
72. Qi X, Liu C, Song L. et al. *PaMADS7*, a MADS-box transcription factor, regulates sweet cherry fruit ripening and softening. *Plant Sci.* 2020;**301**:110634
73. Cai L, Quero-García J, Barreneche T. et al. A fruit firmness QTL identified on linkage group 4 in sweet cherry (*Prunus avium* L.) is associated with domesticated and bred germplasm. *Sci Rep.* 2019;**9**:5008
74. Qi X, Dong Y, Liu C. et al. The *PavNAC56* transcription factor positively regulates fruit ripening and softening in sweet cherry (*Prunus avium*). *Physiol Plant.* 2022b;**174**:e13834
75. Breia R, Mósca AF, Conde A. et al. Sweet cherry (*Prunus avium* L.) *PaPIP1;4* is a functional aquaporin upregulated by pre-harvest calcium treatments that prevent cracking. *Int J Mol Sci.* 2020;**21**:3017
76. Branchereau C, Hardner C, Dirlewanger E. et al. Genotype-by-environment and QTL-by-environment interactions in sweet cherry (*Prunus avium* L.) for flowering date. *Front Plant Sci.* 2023;**14**:1142974
77. Calle A, Cai L, Iezzoni A. et al. Genetic dissection of bloom time in low chilling sweet cherry (*Prunus avium* L.) using a multi-family QTL approach. *Front Plant Sci.* 2020b;**10**:1647
78. Dirlewanger E, Quero-García J, Le Dantec L. et al. Comparison of the genetic determinism of two key phenological traits, flowering and maturity dates, in three *Prunus* species: peach, apricot and sweet cherry. *Heredity (Edinb).* 2012;**109**:280–92
79. Calle A, Grimplet J, Le Dantec L. et al. Identification and characterization of DAMs mutations associated with early blooming in sweet cherry, and validation of DNA-based markers for selection. *Front Plant Sci.* 2021b;**12**:621491
80. Wang J, Gao Z, Li H. et al. Dormancy-associated MADS-box (DAM) genes influence chilling requirement of sweet cherries and co-regulate flower development with *SOC1* gene. *Int J Mol Sci.* 2020c;**21**:921
81. Liu X, Wang J, Sabir IA. et al. *PavGA2ox-2L* inhibits the plant growth and development interacting with *PavDWARF* in sweet cherry (*Prunus avium* L.). *Plant Physiol Biochem.* 2022b;**186**:299–309
82. Wang J, Jiu S, Xu Y. et al. SVP-like gene *PavSVP* potentially suppressing flowering with *PavSEP*, *PavAP1*, and *PavJONITLESS* in sweet cherries (*Prunus avium* L.). *Plant Physiol Biochem.* 2021a;**159**:277–84
83. Wang J, Sun W, Wang L. et al. *FRUITFULL* is involved in double fruit formation at high temperature in sweet cherry. *Environ Exp Bot.* 2022c;**201**:104986
84. Wang L, Sun W, Liu X. et al. Genome-wide identification of the *NCED* gene family and functional characterization of *PavNCED5* related to bud dormancy in sweet cherry. *Sci Hortic.* 2023d;**319**:112186
85. Li Q, Chen P, Dai S. et al. *PacCYP707A2* negatively regulates cherry fruit ripening while *PacCYP707A1* mediates drought tolerance. *J Exp Bot.* 2015;**66**:3765–74
86. Wen Z, Cao X, Hou Q. et al. Expression profiling and function analysis highlight the positive involvement of sweet cherry *PavTCP17* in regulating flower bud dormancy. *Sci Hortic.* 2023;**318**:112138
87. Wang J, Liu X, Sun W. et al. Cold induced genes (CIGs) regulate flower development and dormancy in *Prunus avium* L. *Plant Sci.* 2021b;**313**:111061
88. Ono K, Akagi T, Morimoto T. et al. Genome re-sequencing of diverse sweet cherry (*Prunus avium*) individuals reveals a modifier gene mutation conferring pollen-part self-compatibility. *Plant Cell Physiol.* 2018;**59**:1265–75
89. Li Y, Duan X, Wu C. et al. Ubiquitination of S4-RNase by S-LOCUS F-BOX LIKE2 contributes to self-compatibility of sweet cherry 'Lapins'. *Plant Physiol.* 2020;**184**:1702–16
90. Wang J, Zhang K, Zhang X. et al. Construction of commercial sweet cherry linkage maps and QTL analysis for trunk diameter. *PLoS One.* 2015;**10**:e141261
91. Wu F, Qu D, Zhao X. et al. A high-affinity nitrate transporter *PaNRT2.1* mediates dark septate endophyte (DSE) dependent nitrogen assimilation in sweet cherry roots. *Plant Soil.* 2023a;**489**:539–56
92. Sun Y, Zhao X, Gao Y. et al. Genome-wide analysis of lectin receptor-like kinases (LecRLKs) in sweet cherry (*Prunus avium*) and reveals *PaLectinL16* enhances sweet cherry resistance with salt stress. *Environ Exp Bot.* 2022;**194**:104751
93. Wang Z, Li L, Han J. et al. Combined metabolomics and bioactivity assays kernel by-products of two native Chinese cherry species: the sources of bioactive nutraceutical compounds. *Food Chemistry: X.* 2024;**23**:101625
94. Dirlewanger E, Graziano E, Joobeur T. et al. Comparative mapping and marker-assisted selection in Rosaceae fruit crops. *Proc Natl Acad Sci USA.* 2004;**101**:9891–6
95. Olmstead JW, Sebolt AM, Cabrera A. et al. Construction of an intra-specific sweet cherry (*Prunus avium* L.) genetic linkage map and synteny analysis with the *Prunus* reference map. *Tree Genet Genomes.* 2008;**4**:897–910
96. Gao P, Zheng W, Feng Y. et al. Genetic mapping and QTL analysis for fruit color in sweet cherry using the intra-specific crossing 'Rainier' × '8-100'. *Acta Hortic Sin.* 2012;**39**:135–42
97. Cabrera A, Rosyara UR, De Franceschi P. et al. Rosaceae conserved orthologous sequences marker polymorphism in sweet cherry germplasm and construction of a SNP-based map. *Tree Genet Genomes.* 2012;**8**:237–47
98. Guajardo V, Solís S, Sagredo B. et al. Construction of high density sweet cherry (*Prunus avium* L.) linkage maps using microsatellite markers and SNPs detected by genotyping-by-sequencing (GBS). *PLoS One.* 2015;**10**:e127750
99. Wang D, Karle R, Brettin TS. et al. Genetic linkage map in sour cherry using RFLP markers. *Theor Appl Genet.* 1998;**97**:1217–24
100. Wang D, Karle R, Iezzoni AF. QTL analysis of flower and fruit traits in sour cherry. *Theor Appl Genet.* 2000;**100**:535–44

101. Bošković R, Tobutt KR, Nicoll FJ. Inheritance of isoenzymes and their linkage relationships in two interspecific cherry progenies. *Euphytica*. 1997;**93**:129–43
102. Clarke JB, Sargent DJ, Bošković RI. et al. A cherry map from the inter-specific cross *Prunus avium* 'Napoleon' × *P. nipponica* based on microsatellite, gene-specific and isoenzyme markers. *Tree Genet Genomes*. 2009;**5**:41–51
103. Sooriyapathirana SS, Khan A, Sebolt AM. et al. QTL analysis and candidate gene mapping for skin and flesh color in sweet cherry fruit (*Prunus avium* L.). *Tree Genet Genomes*. 2010;**6**:821–32
104. Hou Q, Li S, Shang C. et al. Genome-wide characterization of chalcone synthase genes in sweet cherry and functional characterization of *CpCHS1* under drought stress. *Front Plant Sci*. 2022;**13**:989959
105. Hou Q, Li X, Qiu Z. et al. Chinese cherry (*Cerasus pseudocerasus* Lindl.) *ARF7* participates in root development and responds to drought and low phosphorus. *Horticulturae*. 2022b;**8**:158
106. Wu F, Qu D, Zhang X. et al. *PaLectinL7* enhances salt tolerance of sweet cherry by regulating lignin deposition in connection with *PaCAD1*. *Tree Physiol*. 2023b;**43**:1986–2000
107. Gao Z, Maurousset L, Lemoine R. et al. Cloning, expression, and characterization of sorbitol transporters from developing sour cherry fruit and leaf sink tissues. *Plant Physiol*. 2003;**131**:1566–75
108. Scheurer S, Pastorello EA, Wangorsch A. et al. Recombinant allergens Pru av 1 and Pru av 4 and a newly identified lipid transfer protein in the in vitro diagnosis of cherry allergy. *J Allergy Clin Immun*. 2001;**107**:724–31
109. Yarur A, Soto E, León G. et al. The sweet cherry (*Prunus avium*) *FLOWERING LOCUS T* gene is expressed during floral bud determination and can promote flowering in a winter-annual *Arabidopsis* accession. *Plant Reprod*. 2016;**29**:311–22
110. Hoyerová K, Perry L, Hand P. et al. Functional characterization of *PaLAX1*, a putative auxin permease, in heterologous plant systems. *Plant Physiol*. 2008;**146**:1128–41